

THEORETICAL COMPUTATION OF THE CHARACTERISTIC  
CURVE OF THE A-C GASEOUS DISCHARGE  
IN AN ELONGATED TUBE

by

CHUNG YOW WANG

B. S., National Taiwan University,  
Taiwan, China, 1952

-----

A THESIS

submitted in partial fulfillment of the  
requirements for the degree

MASTER OF SCIENCE

Department of Electrical Engineering

KANSAS STATE UNIVERSITY  
OF AGRICULTURE AND APPLIED SCIENCE

1959

LD  
2668  
T4  
1959  
W37  
c.2  
Documents

TABLE OF CONTENTS

INTRODUCTION . . . . . 1

THEORY . . . . . 3

    The Model . . . . . 3

    The Formulation of Boundary Value Problem . . . . . 6

    The Difference Method Applied to the Boundary Value  
    Problem . . . . . 12

    The General Procedures of Computation . . . . . 20

RESULTS AND DISCUSSION . . . . . 22

CONCLUSION . . . . . 26

ACKNOWLEDGMENT . . . . . 27

REFERENCES . . . . . 28

APPENDICES . . . . . 29

    APPENDIX I. Constants Used in the Computation . . . 30

    APPENDIX II. Flow Diagram of the Computation Program 31

    APPENDIX III. Computation Program Coded in Fortran  
    Language . . . . . 32

    APPENDIX IV. Solution of Laplace's Equation . . . . 33

SUB-APPENDICES . . . . . 39

    SUB-APPENDIX A. Detail of Derivation of the  
    Equation of Calculation . . . . . 40

    SUB-APPENDIX B. Scheme of the Storage of Function  
    Value . . . . . 43

    SUB-APPENDIX C. Fortran Program of the Laplace  
    Equation . . . . . 48

    SUB-APPENDIX D. Potential Distribution of Each Row  
    of Lattice Points . . . . . 49

    SUB-APPENDIX E. Remarks . . . . . 50

## INTRODUCTION

Theoretical analysis of discharges in gases, because of simplicity, has been limited almost entirely to the one dimensional case, where the electrodes with suitable guard rings were assumed to maintain uniform fields in the planes perpendicular to the line joining the electrodes. An idealized discharge between two infinitely large parallel planes has served to formulate theories concerning various fundamental processes in gaseous discharge. It was used to evaluate coefficients of fundamental importance such as Townsend's first and second coefficients. However, in the study of a relatively long discharge, for example, inter-electrode distances of 50 cm or more, a uniform field requires unusually large electrodes. Such discharges in an elongated tube have been the subject of growing interest for the study and application of plasma energies and plasma oscillations.

Direct-current discharges in elongated tubes have been studied experimentally by many investigators, but theoretical analyses have avoided the use of more than one dimension. As for a-c discharges, McFarland (6) has investigated experimentally the cause of the humidity effect in fluorescent lamps, and McFarland, et al. (7) have completed experimental studies on the striking potential of long low-pressure gaseous discharges, and have deduced empirical formulas.

The development of the modern high-speed electronic digital computer has allowed for the use of numerical methods, previously impractical due to necessary labor. Ward (10) has modified

Crowe, Bragg, and Thomas' numerical method and computed various static characteristics of parallel plate discharges on the SEAC and IBM 704. With various simplifications, i.e., the mobility of ions and electrons was assumed to be constant, the computed curve gave desirable information concerning the discharge, particularly in the region of the glow breakdown corresponding to a negative value for  $dE/dI$ .

The present paper formulates a solution to a problem of an a-c cylindrical glow gaseous discharge. Specifically, the problem was to determine simplified boundary conditions (with reasonably justified assumptions), set up the boundary value problem, and by numerical methods compute the characteristics of instantaneous current versus the potential. Root-mean-square characteristics of a discharge throughout the glow region could then be calculated.

In the computation, the instantaneous potential, ion concentration, and electron concentration were calculated at many regularly spaced points as an intermediate step in computing the current-potential characteristics. Hence the potential, the current wave forms, the space distribution of the field, the charge density, and the current density were immediately obtainable by reasonable modifications of the original computer program when this information was desired.

As the proposed theory of computation has introduced a second space dimension and a time dimension, the nature of the problem and the method of the analysis will be found different from that of Ward, although both methods used the numerical

approach.

In the present paper, the theory is explained. The preliminary computer program is given as an appendix. The major part of the computer program (Laplace's equation) has been solved repeatedly (more than 40 times) in order to find the optimum over-relaxation factor desired in the solution of the linear simultaneous difference equations involved. It is estimated that about 16 hours were required to compute one point of the root-mean-square characteristics on the IBM 650. The time factor and some difficulties met in using the preliminary computer program prevented the final results being given in this paper. This will be discussed in a following section. It is planned to continue this work and to present the revised computer program and results later in a separate paper when successfully computed data is available.

## THEORY

### The Model

A theory was formulated according to the model on Plate I. The diagram shows a section of the cylindrical discharge tube of radius ( $a$ ) and length ( $l$ ) containing two circular disk electrodes made of the same material. The tube wall had a capacitance per unit length ( $C$ ), and the capacitance per unit length between the outside tube wall and the grounded reflector was ( $C'$ ). The surface resistance per unit length along the inside tube wall was

EXPLANATION OF PLATE I

The model of discharge tube.



assumed to be infinitely high, but that of the outside wall was ( $r_0$ ). An external a-c, 60-cycle variable potential was applied to one of the electrodes through a current-limiting resistance ( $R$ ), the other electrode being grounded. The tube was previously evacuated and filled with a low-pressure ( $p$ ) gas.

### The Formulation of Boundary Value Problem

Inside Discharge Body. The theory considered only the existence of one kind of positive ion and electron, along with three fundamental processes--diffusion, mobility, and electron ionization. It ignored recombination, attachment, and other processes, which was justified in the case of low pressure. Within the boundaries, the discharge was governed by a set of three partial differential equations, namely, Poisson's equation (9) and two equations of continuity. (Rationalized MKS units were used throughout this paper.)

$$\nabla^2 U = (N^- - N^+) \frac{e}{\epsilon_0} \quad (1)$$

$$\frac{\partial N^+}{\partial t} = D^+ \nabla^2 N^+ + \nabla \cdot (N^+ \mu^+ \nabla U) + \alpha N^- \quad (2)$$

$$\frac{\partial N^-}{\partial t} = D^- \nabla^2 N^- - \nabla \cdot (N^- \mu^- \nabla U) + \alpha N^- \quad (3)$$

where  $U$  = the potential

$N^+$  = the positive ion concentration

$N^-$  = the electron concentration

$D^+$  = the diffusion constant of positive ions



- $D^-$  = the diffusion constant of electrons  
 $\mu^+$  = the mobility constant of positive ions  
 $\mu^-$  = the electron mobility  
 $\alpha$  = Townsend's first coefficient or electron ionization coefficient.

Boundary Conditions at Wall. Assuming the tube wall to be a perfect recombination place, it was then reasonable to assume  $N^+$  and  $N^-$  to be equal to zero at the wall. Thus the exchange of charge between the wall and the discharge body was only due to diffusion. From the diagram, Plate II, it was possible to obtain the five boundary conditions, namely, equations (4), (5), (6), (7), and (8).

$$\frac{\partial U_1}{\partial z} = r_0 i \quad (4)$$

$$\frac{\partial i}{\partial z} = \frac{\partial(Q_a + Q_b)}{\partial t} \quad (5)$$

$$U_1 = \frac{Q_a}{C'} \quad (6)$$

$$\frac{\partial Q_b}{\partial t} = 2\pi a(D^+ \frac{\partial N^+}{\partial r} - D^- \frac{\partial N^-}{\partial r}) \quad (7)$$

$$U_1 - U_b = \frac{Q_b}{C} \quad (8)$$

Eliminating  $i$ ,  $Q_a$ , and  $Q_b$  from equations (4), (5), (6), and (8), and from (7) and (8), respectively, the following equations resulted:

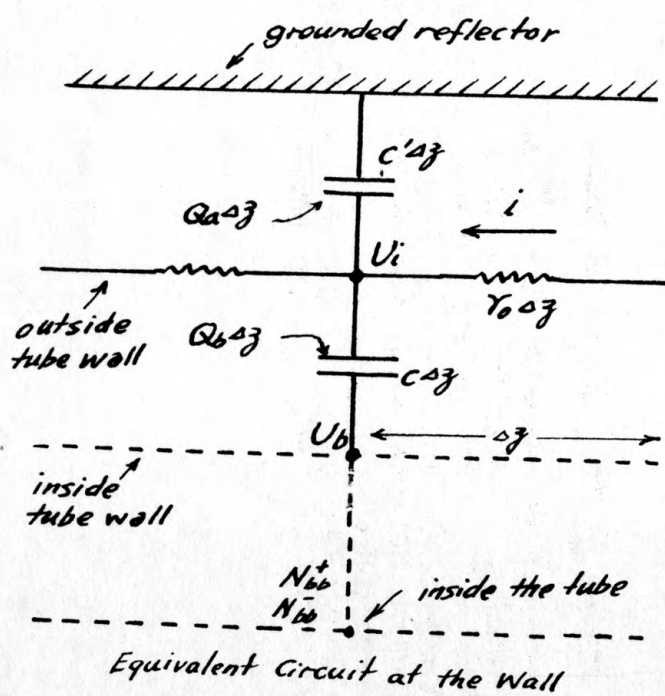
$$(C + C') \frac{\partial U_1}{\partial t} - C \frac{\partial U_b}{\partial t} = \frac{1}{r_0} \frac{\partial^2 U}{\partial z^2} \quad (9)$$

## EXPLANATION OF PLATE II

### Boundary Conditions at Wall

- $U_1$  = the potential at outside tube wall  
 $U_b$  = the potential at inside tube wall  
 $Q_a, Q_b$  = the charge per unit length of the tube wall on the plates indicated in the diagram  
 $i$  = the surface current with direction as indicated in the diagram  
 $N^+_{bb}, N^-_{bb}$  = the ion and electron density at one  $k$  distance from the inside tube wall.

## PLATE II



$$C \frac{\partial U_1}{\partial t} - C \frac{\partial U_b}{\partial t} = 2\pi a (D^+ \frac{\partial N^+}{\partial r} - D^- \frac{\partial N^-}{\partial r}) \quad (10)$$

Solving for  $U_1$  and  $U_b$ , the final boundary conditions are:

$$C' \frac{\partial U_1}{\partial t} = \frac{1}{r_0} \frac{\partial^2 U_1}{\partial z^2} - 2\pi a (D^+ \frac{\partial N^+}{\partial r} - D^- \frac{\partial N^-}{\partial r}) \quad (11)$$

$$C' \frac{\partial U_b}{\partial t} = \frac{1}{r_0} \frac{\partial^2 U_1}{\partial z^2} - \frac{2\pi a (C + C')}{C} (D^+ \frac{\partial N^+}{\partial r} - D^- \frac{\partial N^-}{\partial r}) \quad (12)$$

Boundary Conditions at Electrodes. After an a-c potential was applied through the resistance  $R$  to the discharge tube, the potential of the ungrounded electrode was given by equation (13).

$$U_e = U_m \sin(120 \pi t) - IR \quad (13)$$

where  $U_m$  = the maximum value of the applied a-c potential

$I$  = the total instantaneous current in the external circuit.

At the cathode, the positive ion density was obtained by using parabolic extrapolation from the values at nearby points equidistant from the axis of the cylindrical tube. This extrapolation yielded

$$N_c^+ = 3(N_{1c}^+ - N_{2c}^+) + N_{3c}^+ \quad (14)$$

where  $N_c^+$  = the ion density at cathode

$N_{1c}^+$ ,  $N_{2c}^+$ ,  $N_{3c}^+$  = the ion density at  $1h$ ,  $2h$ , and  $3h$  distance horizontally from cathode respectively.

This was based on the assumption that the ion density is a continuous function of space. The glow discharge has been described by von Engel (2) as a discharge in which the cathode emits electrons under the bombardment of positive ions, metastable atoms, and light quanta from the gas. The thermionic emission in the

cold-cathode case is negligible. Combining the above three emission causes under a pseudo-Townsend's second coefficient  $\gamma$ , the electron density may be expressed in terms of positive ion density (equation 16). This requires that in current density term, diffusion be neglected in comparison with mobility, and the initial velocity of the emitted electron be ignored.

$$N_c^- \mu^- |E_c| = \gamma N_c^+ \mu^+ |E_c| \quad (15)$$

$$N_c^- = \gamma \frac{\mu^+}{\mu^-} N_c^+ \quad (16)$$

where  $N_c^-$  = the electron density at cathode

$E_c$  = the electric field at cathode

$\gamma$  = the pseudo-Townsend's second coefficient.

At the anode, the continuity condition requires that the ion density must vanish  $N_a^+ = 0$  (8). If continuity conditions were imposed on the electrodes so that the total current density (due to ions and electrons) at one point of the cathode were equal to that of the corresponding point of the anode, then the electron density at the anode is given by equation (18).

$$N_a^- \mu^- |E_a| = (1 + \gamma) N_c^+ \mu^+ |E_c| \quad (17)$$

$$N_a^- = \frac{(1 + \gamma) \mu^+}{\mu^-} \frac{|E_c|}{|E_a|} N_c^+ \quad (18)$$

where  $N_a^-$  = the electron density at anode

$E_a$  = the electric field at anode.

In deriving the above equations, it was understood that the longitudinal component of the field was unidirectional, from anode to cathode, in the discharge tube.

Finally, the total instantaneous current in the external

circuit can be expressed by the following equation:

$$I = 2 \pi e \int_0^a N^-_a r dr \quad (19)$$

Initial Conditions. Before the potential was applied to the discharge tube, the ion and electron densities due to cosmic ionization were assumed to be  $5 \times 10^8$  particles per cubic meter, which were minimum values given by von Engel (2) for sea level. At wall and electrodes, electron and ion densities were assumed to be zero.

#### The Difference Method Applied to the Boundary Value Problem

The above formulated boundary value problem can be computed and solved step by step if the approximation of finite differences is used. In the case of cylindrical symmetry, equations (1), (2), and (3) became:

$$\frac{\partial^2 U}{\partial r^2} + \frac{1}{r} \frac{\partial U}{\partial r} + \frac{\partial^2 U}{\partial z^2} = (N^- - N^+) \frac{e}{\epsilon_0} \quad (1')$$

$$\begin{aligned} \frac{\partial N^+}{\partial t} = D^+ & \left( \frac{\partial^2 N^+}{\partial r^2} + \frac{1}{r} \frac{\partial N^+}{\partial r} + \frac{\partial^2 N^+}{\partial z^2} \right) \\ & + N^+ \mu^+ \left( \frac{\partial^2 U}{\partial r^2} + \frac{1}{r} \frac{\partial U}{\partial r} + \frac{\partial^2 U}{\partial z^2} \right) \\ & + \mu^+ \left[ \frac{\partial U}{\partial r} \frac{\partial N^+}{\partial r} + \frac{\partial N^+}{\partial r} \frac{\partial U}{\partial r} + \frac{\partial U}{\partial z} \frac{\partial N^+}{\partial z} + \frac{\partial N^+}{\partial z} \frac{\partial U}{\partial z} \right] + \alpha N^- \quad (2') \end{aligned}$$

$$\begin{aligned}
\frac{\partial N^-}{\partial t} = & D^- \left( \frac{\partial^2 N^-}{\partial r^2} + \frac{1}{r} \frac{\partial N^-}{\partial r} + \frac{\partial^2 N^-}{\partial z^2} \right) \\
& - N^- \mu^- \left( \frac{\partial^2 U}{\partial r^2} + \frac{1}{r} \frac{\partial U}{\partial r} + \frac{\partial^2 U}{\partial z^2} \right) \\
& - \mu^- \left[ \frac{\partial U}{\partial r} \frac{N^-}{r} + \frac{\partial N^-}{\partial r} \frac{\partial U}{\partial z} + \frac{\partial U}{\partial z} \frac{\partial N^-}{\partial z} \right] + \alpha N^- \quad (3')
\end{aligned}$$

Because of symmetry, the discharge region may be represented by a rectangular section with the center line and wall as two horizontal sides. The electrodes are the two lateral sides. This section was divided into a rectangular net, as shown on Plate III, where one line was added below the center line as a necessity for programming and two lines were added above the line of the wall to take account of the outside wall and the reflector.

For each row of lattice points, the equations (1'), (2'), and (3') were different. But if variable coefficients depending on (j), the row number (as shown on Plate III), were used, the above three equations could then be transformed into three sets of difference equations. For the first row,  $l'$  Hospital Rule enables use of  $\frac{\partial}{\partial r}$  and  $\frac{\partial^2}{\partial r^2}$  to approximate  $\frac{1}{r}$  and  $\frac{1}{r} \frac{\partial}{\partial r}$ , respectively, since for  $r \rightarrow 0$ , the latter are undefined.

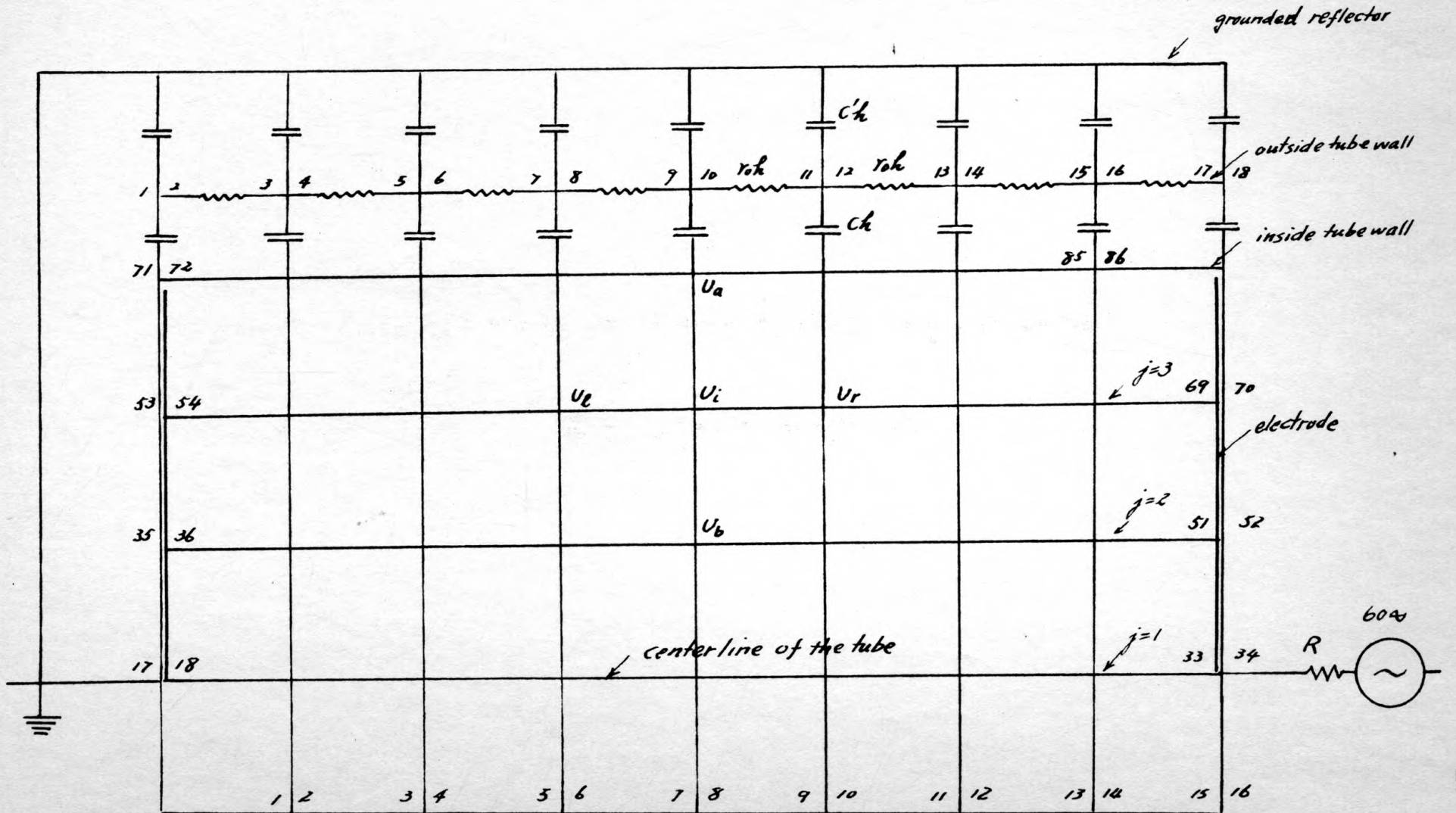
The above considerations, and use of central differences, result in difference equations that can be reduced to equations (20), (21), and (22), where subscripts (a), (b), (r), ( $l$ ), and (i) denote the points above, below, to the right, to the left, and the point itself.  $A_{ji}$ , etc.,  $G_j$  and  $B_{2j}, B_{3j}$  were functions of row number and the net size, h and k, as shown on Plate IV.

EXPLANATION OF PLATE III

Net diagram of the discharge region and boundaries.



PLATE III



EXPLANATION OF PLATE IV

Coefficients of equations (20), (21),  
and (22).

## PLATE IV

	$i=1$	$i=2$	$i=3$	$i=4$	$i=5$
$A_{1i}$	$\frac{2h^2}{2h^2+h^2}$	$\frac{4D^-}{h^2}$	$\frac{4D^+}{h^2}$	$-\frac{4\mu^-}{h^2}$	$\frac{4\mu^+}{h^2}$
$A_{2i}$	$\frac{3h^2}{4(h^2+h^2)}$	$\frac{3D^-}{2h^2}$	$\frac{3D^+}{2h^2}$	$-\frac{3\mu^-}{2h^2}$	$\frac{3\mu^+}{2h^2}$
$A_{3i}$	$\frac{5h^2}{8(h^2+h^2)}$	$\frac{5D^-}{4h^2}$	$\frac{5D^+}{4h^2}$	$-\frac{5\mu^-}{4h^2}$	$\frac{5\mu^+}{4h^2}$
$B_{1i}$	0	0	0	0	0
$B_{2i}$	$\frac{h^2}{4(h^2+h^2)}$	$\frac{D^-}{2h^2}$	$\frac{D^+}{2h^2}$	$-\frac{\mu^-}{2h^2}$	$\frac{\mu^+}{2h^2}$
$B_{3i}$	$\frac{3h^2}{8(h^2+h^2)}$	$\frac{3D^-}{4h^2}$	$\frac{3D^+}{4h^2}$	$-\frac{3\mu^-}{4h^2}$	$\frac{3\mu^+}{4h^2}$
$C_{1i}$	$\frac{h^2}{2(2h^2+h^2)}$	$\frac{D^-}{h^2}$	$\frac{D^+}{h^2}$	$-\frac{\mu^-}{h^2}$	$\frac{\mu^+}{h^2}$
$C_{2i}$	$\frac{h^2}{2(h^2+h^2)}$	"	"	"	"
$C_{3i}$	"	"	"	"	"
$D_{1i}$	$\frac{1-w}{w}$	$\frac{-2(2h^2+h^2)D^-}{h^2h^2}$	$\frac{-2(2h^2+h^2)D^+}{h^2h^2}$	$\frac{2(2h^2+h^2)\mu^-}{h^2h^2}$	$\frac{-2(2h^2+h^2)\mu^+}{h^2h^2}$
$D_{2i}$	"	$\frac{-2(h^2+h^2)D^-}{h^2h^2}$	$\frac{-2(h^2+h^2)D^+}{h^2h^2}$	$\frac{2(h^2+h^2)\mu^-}{h^2h^2}$	$\frac{-2(h^2+h^2)\mu^+}{h^2h^2}$
$D_{3i}$	"	"	"	"	"
$B_{2j}$	0	$\frac{1}{h}$	$\frac{1}{2h}$		
$B_{3j}$	0	$\frac{1}{2h}$	$\frac{1}{2h}$		
$G_{ij}$	$\frac{h^2h^2}{2(2h^2+h^2)}$	$\frac{h^2h^2}{2(h^2+h^2)}$	$\frac{h^2h^2}{2(h^2+h^2)}$		

$$A_{j1}U_a + B_{j1}U_b + C_{j1}(U_r + U_\ell) + D_{j1}U_i \\ = G_j(N_i^- - N_i^+) \frac{e}{\epsilon_0} \quad (20)$$

$$i = 19, 21 \dots 67 \text{ or } 20, 22 \dots 68$$

$$j = 1, 2, 3$$

$$\begin{aligned} \frac{\Delta N_i^+}{\Delta t} &= \left[ A_{j3}N_a^+ + B_{j3}N_b^+ + C_{j3}(N_r^+ + N_\ell^+) + D_{j3}N_i^+ \right] \\ &+ N_i^+ \left[ A_{j5}U_a + B_{j5}U_b + C_{j5}(U_r + U_\ell) + D_{j5}U_i \right] \\ &+ \mu^+ \left[ \frac{1}{2k} (U_a - U_b) \{ B_{2j}N_i^+ + B_{3j}(N_a^+ - N_b^+) \} \right. \\ &\left. + \frac{1}{4h^2} (U_r - U_\ell) (N_r^+ - N_\ell^+) \right] + \alpha N_i^- \quad (21) \end{aligned}$$

$$\begin{aligned} \frac{\Delta N_i^-}{\Delta t} &= \left[ A_{j2}N_a^- + B_{j2}N_b^- + C_{j2}(N_r^- + N_\ell^-) + D_{j2}N_i^- \right] \\ &+ N_i^- \left[ A_{j4}U_a + B_{j4}U_b + C_{j4}(U_r + U_\ell) + D_{j4}U_i \right] \\ &- \mu^- \left[ \frac{1}{2k} (U_a - U_b) \{ B_{2j}N_i^- + B_{3j}(N_a^- - N_b^-) \} \right. \\ &\left. + \frac{1}{4h^2} (U_r - U_\ell) (N_r^- - N_\ell^-) \right] + \alpha N_i^- \quad (22) \end{aligned}$$

$\alpha$  was computed by the following equation (Ward, 10):

$$\alpha = C p e^{-D\sqrt{P/E}} \quad (23)$$

$$E = \sqrt{\frac{1}{4k^2} (U_a - U_b)^2 + \frac{1}{4h^2} (U_r - U_\ell)^2} \quad (24)$$

where  $C, D =$  constants for the gas used

$p =$  gas pressure.

The boundary conditions, equations (11) and (12), became:

$$\frac{\Delta U_i}{\Delta t} = C_1(U_r + U_\ell - 2U_i) + C_2N_{bb}^+ - C_3N_{bb}^- \quad (25)$$

$$\frac{\Delta U_b}{\Delta t} = C_1(U_r + U_l - 2U_1) + C_4(C_2 N_{bb}^+ - C_3 N_{bb}^-) \quad (26)$$

where  $N_{bb}^-$ ,  $N_{bb}^+$  were the values of  $N^-$  and  $N^+$  at  $j = 3$ , or at the second row below the row of  $U_1$ , and

$$C_1 = \frac{\Delta t}{C' h^2 r_0}$$

$$C_2 = \frac{2 \pi a e D^+ \Delta t}{C' k}$$

$$C_3 = \frac{2 \pi a e D^- \Delta t}{C' k}$$

$$C_4 = (C + C')/C$$

The boundary value of  $U$  at the end points of the wall were obtained by extrapolation from the nearby boundary values of  $U$ .

The boundary conditions at electrodes became:

$$N^+_{cj} = 3(N^+_{1cj} - N^+_{2cj}) + N^+_{3cj} \quad (27)$$

$$N^-_{cj} = \delta \frac{\mu^+}{\mu^-} N^+_{cj} \quad (28)$$

$$N^+_{aj} = 0 \quad (29)$$

$$N^-_{aj} = \frac{(1 + \delta) \mu^+}{\mu^-} \frac{|E_c|}{|E_a|} \cdot N^+_{cj} \quad (30)$$

$$U_e = U_m \sin(120 \pi n \Delta t) - IR \quad (31)$$

where the subscript  $j$  denotes the row number and runs from 1 to 3. For example, in  $N^+_{3c2}$ , the subscript before  $c$  means the distance from the cathode horizontally in terms of net size  $h$ , and the one following  $c$  means the row number. Thus it is the positive ion density on the second row and  $3h$  distance from the cathode. The small  $n$  is an integer.

The total instantaneous current in the external circuit was

computed by the following approximation. For  $0 < r < \frac{k}{2}$ ,  $\frac{k}{2} < r < \frac{3k}{2}$ ,  $\frac{3k}{2} < r < \frac{5k}{2}$ , and  $\frac{5k}{2} < r < 3k$ , use  $N_{a1}^-$ ,  $N_{a2}^-$ ,  $N_{a3}^-$ , and 0 as their average electron density. Thus

$$I_a^- = \frac{\pi}{4} k^2 e \mu^- E_{a1} N_{a1}^- + 2\pi k^2 e \mu^- E_{a2} N_{a2}^- + 4\pi k^2 e \mu^- E_{a3} N_{a3}^- \quad (32)$$

### The General Procedures of Computation

The original boundary value problem consisted of a set of partial differential equations involving ion density, electron density, and potential as functions of three independent arguments: radial distance ( $r$ ), longitudinal distance ( $z$ ), and time ( $t$ ). After using the method of finite differences, this set of partial differential equations became a set of difference equations. These latter equations may be divided into two parts, involving or not involving time explicitly. A set of linear simultaneous equations resulted, in which there were as many equations as there were unknowns. Therefore a step-by-step calculation may be followed by dividing time into small intervals of  $\Delta t$ . Knowing the initial conditions, the time dependent part was calculated to get the new value of the function for an increment of time  $\Delta t$ . Then the other simultaneous equation part was solved by the over-relaxation method. This same procedure was repeated for another increment of time  $\Delta t$ , and so on. Thus the instantaneous voltage and current were obtained, and the root-mean-square characteristics were computed.

The preceding section furnished all the equations that were needed for computing the solution of the problem. The following were the procedures followed by the computer program (see Appendix III) designed for use on the IBM 650.

1. Set initial conditions at  $t = 0$ , before the potential is applied.
2. Calculate the boundary value of  $U$  at inner points at wall for  $t = \Delta t$ , by equations (25) and (26).
3. Extrapolate the new value of  $U$  at nearby inner points at wall to get the  $U$  at the end points of wall for  $t = \Delta t$ .
4. Calculate  $U_0$  at the ungrounded electrode by equation (31).
5. Use scanning calculations iteratively (an over-relaxation method) to approach successively the solution of the linear simultaneous equation (20), i.e., to find the region values of  $U$  for  $t = \Delta t$ .
6. Calculate  $\Delta N^-$  by equation (22), and obtain the new value of  $N^-$  by  $N'^- = N^- + \Delta N^-$ . This does not include the new boundary value at electrodes.
7. Do the same thing for  $N^+$ , using equation (21).
8. Extrapolate the new value of  $N^+$  nearby the cathode to get  $N^+_{cj}$ , by equation (27), and obtain  $N^-_{cj}$ ,  $N^-_{aj}$  by equations (28) and (30), respectively. Set  $N^+_{aj} = 0$ . All these were done after the determination of the half cycle (+ or -) of the applied potential.
9. Calculate the total instantaneous current in the external circuit by equation (32).

Repeat the above procedures for another  $\Delta t$ , etc.

## RESULTS AND DISCUSSION

The above formulated theory was complete in itself. A computer program has been designed in Fortran Language (see Appendix III), so that it may be accepted by either the IBM 650 or 704 computer. This program has been processed to the object program of machine language by the revised (1958) For Transit II system on the IBM 650. The object program functioned exactly as it was designed. The time-consuming part of the program was Poisson's equation. A special case of this equation, namely, Laplace's equation, has been solved separately as a preliminary part of this study many times with different degrees of accuracy and relaxation factors on the IBM 650. The relations of the number of iterated calculations required versus relaxation factor ( $\omega$ ) and degree of accuracy ( $S_j$ ) were plotted on Plate V. The details of the Laplace calculations are given in Appendix IV.

From the curves, it was seen that there was an optimum relaxation factor of 1.4, which seemed to be constant for various degrees of accuracy. For a specific relaxation factor the number of iterations is proportional to the logarithm of the degree of accuracy. Thus a high degree of accuracy of the solution to the simultaneous equation could be obtained by increasing a few additional iterations of calculation.

The curves also showed that for the optimum case, not only



EXPLANATION OF PLATE V

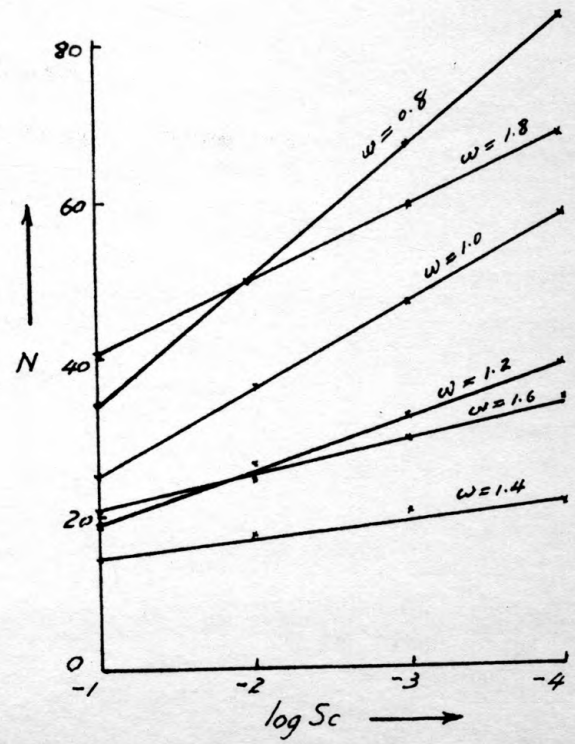
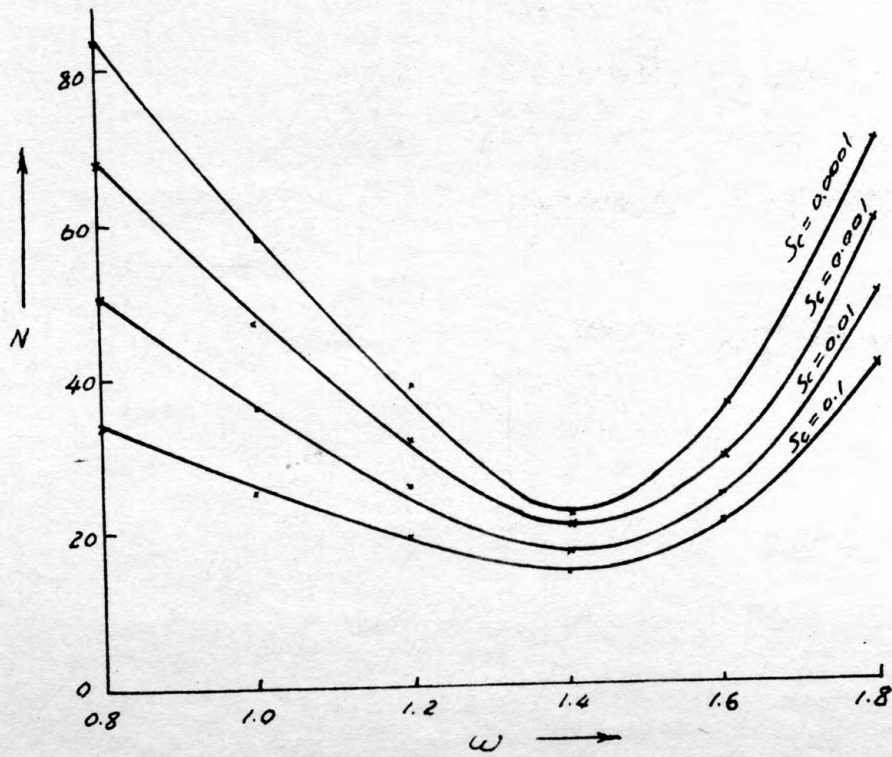
Relaxation efficiency curves.

$S_c$  = degree of accuracy or convergence criterion

$N$  = number of iterated calculations

$\omega$  = relaxation factor

PLATE V



the starting point is low but the slope is also small. That meant the successive scanning calculations converged to the solution of the problem faster than at any other relaxation factor, both at the beginning and at the later phases. For two relaxation factors which are equally apart from the optimum factor from each side, the figure showed the smaller one corresponded to a calculation which converged faster at the beginning but slowed down later at high accuracy. On the other hand, the larger one corresponded to a calculation converging slowly at the beginning but fast toward the high accuracy. Thus a rough conclusion may be drawn: to seek high accuracy solution, a larger relaxation factor might be used; otherwise the smaller one is better.

The voltage characteristics have not been obtained. After  $2\Delta t$ , during the solution of the simultaneous equations (Poisson's equation), the iterated calculation diverged instead of converging to the proper solution. It was found that  $N^-$  and  $N^+$  became negative, which was absurd, and the potential at the wall oscillated between + and - along the z-direction. The possible causes may be that the constants ( $D^+$ ,  $D^-$ , etc.) used in the program were not appropriately chosen, or the boundary conditions at the wall were overly simplified, i.e.,  $N^+$  and  $N^-$  were not zero at wall and mobility current to the wall should be taken into account.

Additional work is in progress for improving this result.

## CONCLUSION

The success in solving Laplace's equation in cylindrical coordinates on the IBM 650 computer and the first two calculations following the present computer program, showed that the approach chosen was adequate in computing the voltage characteristics of the cylindrical gaseous discharge. Based on the present theory and the computation program, an adjustment of constants and modification of the boundary condition were believed to be sufficient to solve the difficulty that impeded the computation.

The IBM 650 computer, because of its storage and speed limitations, is not suitable to solve the present problem. A bigger and faster machine such as the IBM 704 would be more appropriate for this work.

## ACKNOWLEDGMENTS

It is with gratitude that the author wishes to acknowledge the assistance the following people gave him, for without their help this paper could not have been completed: Dr. R. H. McFarland, of the Department of Physics, for his guidance, suggestions, and patience in correcting the thesis; Dr. A. B. Cardwell, Head of the Department of Physics, for his help and encouragement; Dr. C. A. Halijak, of the Department of Electrical Engineering, and Professor R. M. Kerchner, Head of the Department of Electrical Engineering, for their assistance and aid; Dr. S. E. Whitcomb, the former Head of the Department of Physics, for placing him in a position through which he was able to attain his goal; Dr. S. T. Parker and Mr. T. L. Hamilton, Director and Assistant Director of the IBM Center, for suggesting the methods needed in solving the mathematical problems involved, demonstrating the use of the IBM machine, and allowing him to use the machine when necessary; Dr. P. G. Kirmser, of the Department of Applied Mechanics, for his suggestions in the numerical method used in the thesis; Mr. Raimo Bakis, graduate student in Physics, for assisting with ideas for the thesis; Mr. S. C. Chang, graduate student in Physics, who assisted with the corrections necessary; and the author's wife, Helen Chen-Wang, and her friend, Mrs. D. Del Vecchio, who took the time for editing this paper.

The author also wishes to express his appreciation to the sponsors of the author's research project, the Office of Ordnance Research, United States Army.

## REFERENCES

- (1) Brown, S. C. and W. P. Allis.  
Basic data of electrical discharges. Technical Report No. 283, Research Laboratory of Electronics, M.I.T., Cambridge, Mass., June, 1954.
- (2) Engel, A. von.  
Ionized gases. Oxford: Clarendon Press, 1955.
- (3) Flugge, S.  
Encyclopedia of physics. Berlin: Gottingen. Heidelberg: Springer-Verlog, 21-22, 1956.
- (4) Kunz, K. S.  
Numerical analysis. New York, Toronto, London: McGraw-Hill, 1957.
- (5) Loeb, L. B.  
Basic processes of gaseous electronics. Berkeley and Los Angeles: University of California Press, 1955.
- (6) McFarland, R. H.  
The cause of the humidity effect in fluorescent lamps. Illuminating Engineering, 46:345-349, July, 1951.
- (7) McFarland, R. H., C. A. Bell, J. Ladesich, R. A. Anderson, and R. Bakis.  
Striking potentials of long, low pressure mercury-argon electric discharges. Illuminating Engineering, 52:417-420, Aug., 1957.
- (8) Newton, R. R.  
Transients in Townsend discharges. Phys. Rev., 73: 570-583, March, 1948.
- (9) Prudkovskaia, O. V. and M. F. Shirokov.  
On the theory of stationary striations in the positive column of a gas discharge. Soviet Physics "Doklady", 2-1:96-99, Jan.-Feb., 1957.
- (10) Ward, A. L.  
Effect of space charge formation upon electrical breakdown in gases. Report of Diamond Ordnance Fuze Laboratories, Ordnance Corps, Department of the Army, TR-500, Aug., 1957.
- (11) Young, D. and F. Lerch.  
The numerical solution of Laplace's equation on ORDVAC. Memorandum Report No. 708, Ballistic Research Lab., Aberdeen Proving Ground, Maryland, July, 1953.

**APPENDICES**

## APPENDIX I

## Constants Used in the Computation

The following constants were chosen from the practical viewpoint:

$l = 0.05$  m (this was limited by the computer storage places of the IBM 650)

$a = 0.0183$  m (this was the radius of the actual discharge tube the author was working on)

$$C = 2\pi \epsilon l n \frac{b}{a} = 2\pi \epsilon l n \frac{41}{39} = 2.0 \times 10^{-11} \text{ F/m}$$

$$C' = C$$

$\omega = 1.4$  (over-relaxation factor)

$p = 10$  mm of Hg

$R = 1000$  ohms

The following constants were rounded figures taken or calculated from the sources listed:

$D^+ = 4.7 \times 10^{-3}$  m<sup>2</sup>/sec for A<sup>+</sup> p = 10 mm of Hg (2, p. 119)

$D^- = 5$  m<sup>2</sup>/sec for A<sup>+</sup> p = 10 mm of Hg (2, p. 119)

$\mu^+ = 1.5 \times 10^{-3}$  m<sup>2</sup>/sec/V for A<sup>+</sup> p = 10 mm of Hg (5, p. 100)

$\mu^- = 3$  m<sup>2</sup>/sec/V for A<sup>+</sup> p = 10 mm of Hg (5, p. 100)

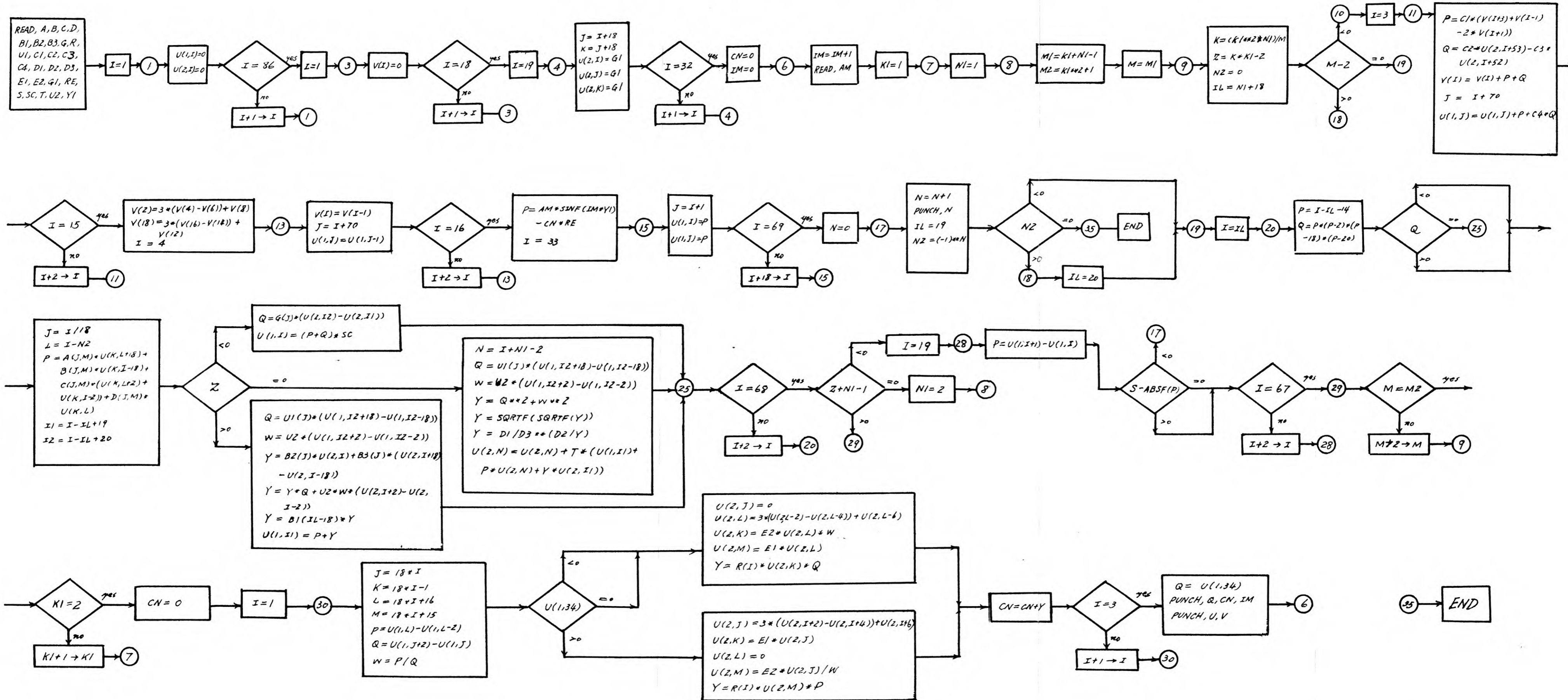
$\gamma = 0.02$  for N<sub>1</sub> - A<sup>+</sup> (1, p. 31)

$C_p = 316 \times 10^2$  (5, p. 692-695)

$D_p = 86$  (5, p. 692-695)

$r_0 = 1 \times 10^6$  ohms/m (6)





## APPENDIX III

## Computation Program Coded in Fortran Language

```

000000 PØISSIØN EQUATIØN
000000 DIMENSIØN B1(2),B2
000001 (3),B3(3),G(3),R(3),
000002 U1(3),V(18),A(3,5),
000003 B(3,5),C(3,5),D(3,5
000004 ),U(2,86)
000000 READ,A,B,C,D
000000 READ,B1,B2,B3,G,R,U1
000000 READ,C1,C2,C3,C4,
000001 D1,D2,D3,E1,E2
000000 READ,G1,RE,
000001 S,SC,T,U2,Y1
000000 DØ2 I=1,86
000010 U(1,I)=0.0
000020 U(2,I)=0.0
000000 DØ3 I=1,18
000030 V(I)=0.0
000000 DØ5 I=19,32
000040 J=I+18
000000 K=J+18
000000 U(2,I)=G1
000000 U(2,J)=G1
000050 U(2,K)=G1
000000 CN=0.0
000000 IM=0
000060 IM=IM+1
000000 READ,AM
000000 DØ29 K1=1,2
000070 N1=1
000080 M1=K1+N1-1
000000 M2=K1**2+1
000000 DØ29 M=M1,M2,2
000090 K=(K1**2*N1)/M
000000 Z=K*K1-2
000000 N2=0
000000 IL=N1+18
000000 IF(M-2)10,19,18
000100 DØ12 I=3,15,2
000110 P=C1*(V(I+3)+V(I-1)
000111 -2*V(I+1))
000000 Q=C2*U(2,I+53)-C3*
000001 U(2,I+52)
000000 V(I)=V(I)+P+Q
000000 J=I+70
000120 U(1,J)=U(1,J)+P+C4*Q
000000 V(2)=3*(V(4)-V(6))
000001 +V(8)
000000 V(18)=3*(V(16)-V(14)
000001 )+V(12)
000000 DØ14 I=4,16,2
000130 V(I)=V(I-1)
000000 J=I+70
000140 U(1,J)=U(1,J-1)
000000 P=AM*SINF(IM*Y1)
000001 -CN*RE
000000 DØ16 I=33,69,18
000150 J=I+1
000000 U(1,I)=P
000160 U(1,J)=P
000000 N=0
000170 N=N+1
000000 PUNCH,N
000000 IL=19
000000 N2=(-1)**N
000000 IF(N2)19,35,18
000180 IL=20
000190 DØ25 I=IL,68,2
000200 P=I-IL-14
000000 Q=P*(P-2)*(P-18)*
000001 (P-20)
000000 IF(Q)21,25,21
000210 J=I/18
000000 L=I-N2
000000 P=A(J,M)*U(K,L+18)+
000001 B(J,M)*U(K,I-18)
000000 P=P+C(J,M)*(U(K,L+2)
000001 +U(K,I-2))
000000 P=P+D(J,M)*U(K,L)
000000 I1=I-IL+19
000000 I2=I-IL+20
000000 IF(Z)22,24,23
000220 Q=G(J)*(U(2,I2)-U
000221 (2,I1))
000000 U(1,I)=(P+Q)*SC
000000 GØ TØ 25
000230 Q=U1(J)*(U(1,I2+18)-
000231 U(1,I2-18))
000000 W=U2*(U(1,I2+2)-
000001 U(1,I2-2))
000000 Y=B2(J)*U(2,I)+B3(J)
000001 *(U(2,I+18)-U(2,I-
000002 18))
000000 Y=Y*Q+U2*W*(
000001 U(2,I+2)-U(2,I-2))
000000 Y=B1(IL-18)*Y
000000 U(1,I1)=P+Y
000000 GØ TØ 25
000240 N=I+N1-2
000000 Q=U1(J)*(U(1,I2+18)-
000001 U(1,I2-18))
000000 W=U2*(U(1,I2+2)-
000001 U(1,I2-2))
000000 Y=Q**2+W**2
000000 Y=SQRTF(Y)
000000 Y=SQRTF(Y)
000000 Y=D1/D3**(D2/Y)
000000 U(2,N)=U(2,N)+T*
000001 (U(1,I1)+P*U(2,N)+
000002 Y*U(2,I1))
000250 CØNTINUE
000000 IF(Z+N1-1)27,26,29
000260 N1=2
000000 GØ TØ 8
000270 DØ29 I=19,67,2
000280 P=U(1,I+1)-U(1,I)
000000 IF(S-ABS(P))17,
000001 29,29
000290 CØNTINUE
000000 CN=0.0
000000 DØ33 I=1,3
000300 J=18*I
000000 K=18*I-1
000000 L=18*I+16
000000 M=18*I+15
000000 P=U(1,L)-U(1,L-2)
000000 Q=U(1,J+2)-U(1,J)
000000 W=P/Q
000000 IF(U(1,34))31,31,32
000310 U(2,J)=0.0
000000 U(2,L)=3*(U(2,L-2)-
000001 U(2,L-4))+U(2,L-6)
000000 U(2,K)=E2*U(2,L)*W
000000 U(2,M)=E1*U(2,L)
000000 Y=R(I)*U(2,K)*Q
000000 GØ TØ 33
000320 U(2,J)=3*(U(2,J+2)-
000321 U(2,J+4))+U(2,J+6)
000000 U(2,K)=E1*U(2,J)
000000 U(2,L)=0.0
000000 U(2,M)=E2*U(2,J)/W
000000 Y=R(I)*U(2,M)*P
000330 CN=CN+Y
000000 Q=U(1,34)
000340 PUNCH,Q,CN,IM
000000 PUNCH,U,V
000000 GØ TØ 6
000350 END

```

## APPENDIX IV

## Solution of Laplace's Equation

Laplace's equation in cylindrical coordinates was solved as a boundary value problem by using numerical techniques on the IBM 650 computer. The results obtained showed the optimum relaxation factor used in solving the difference equations involved is approximately 1.4, which is constant for various degrees of accuracy for this particular configuration and various numbers of lattice points used. The accuracy of the solution of the resulted difference equations increases geometrically while the numbers of iterated calculation required increases only arithmetically. Thus reasonable accuracy could be obtained by a relatively small increase of machine time consumption.

Problem. In a cylindrical space of radius  $a$  and length  $l$ , if the function to be found is independent of polar angle  $\theta$ , the Laplace equation is reduced to the following form:

$$\nabla^2 U = \frac{\partial^2 U}{\partial r^2} + \frac{1}{r} \frac{\partial U}{\partial r} + \frac{\partial^2 U}{\partial z^2} = 0 \quad (1)$$

Passing a cross section through the center line of the cylinder, and dividing one-half of this section into a net as shown in Fig. 1, one obtains a two-dimensional region with 40 interior lattice points. Numerical methods will be used to solve equation (1), for proper boundary conditions, at each of these points.

Preparation of the Problem for Using the Computer. By the use of central differences, at lattice points not on the center

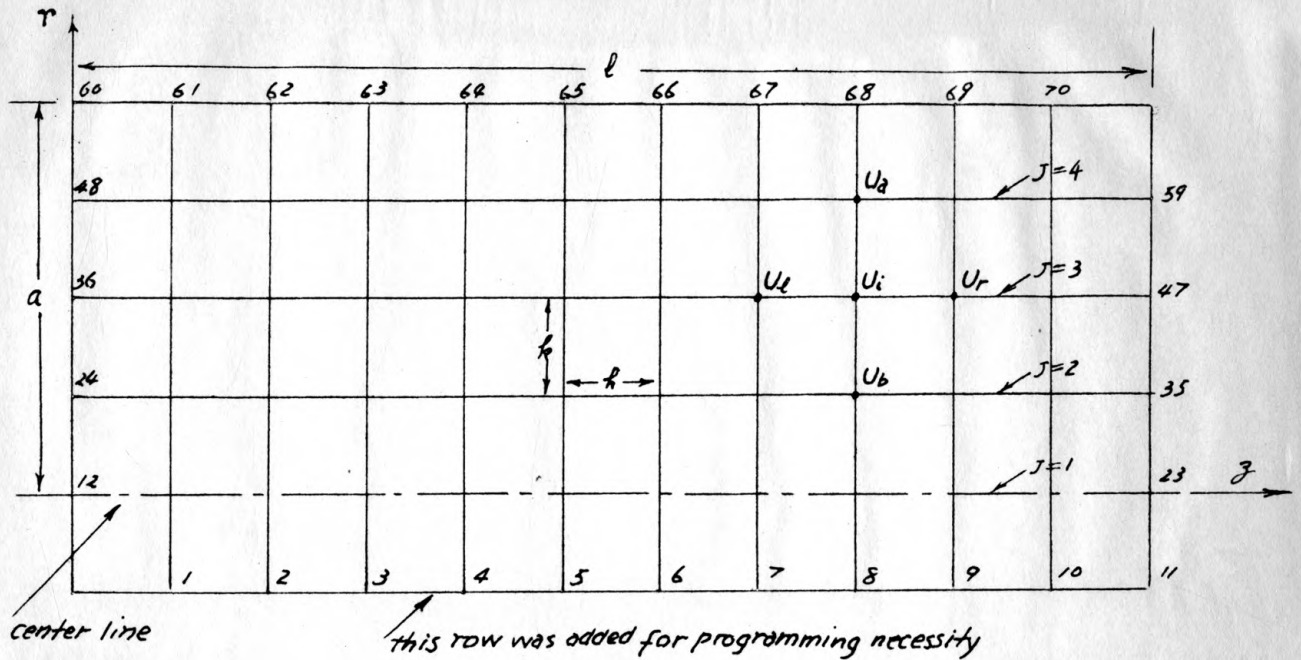


Fig. 1. Net diagram for 40 interior points.

line, the Laplace equation is approximated by the following equation:

$$\begin{aligned}
 (\nabla^2 U)_i &= \frac{1}{k^2} (U_a - 2U_i + U_b) + \frac{1}{2(J-1)k^2} (U_a - U_b) \\
 &+ \frac{1}{h^2} (U_r - 2U_i + U_l) \quad (2) \\
 i &= 13 \dots 58
 \end{aligned}$$

where  $J$  is the interior row number of the  $i$ th lattice point,  $2 \leq J \leq 4$ . At each lattice point on the center line,  $r = 0$ ,

the limiting value of  $\frac{1}{r} \frac{\partial U}{\partial r}$  may be used,

$$\lim_{r \rightarrow 0} \frac{1}{r} \frac{\partial U}{\partial r} = \frac{\frac{\partial}{\partial r} \left( \frac{\partial U}{\partial r} \right)}{\frac{\partial}{\partial r} (r)} = \frac{\partial^2 U}{\partial r^2}$$

since in most physical problems the function could not have singular points on the center line and the saddle point possibility is ruled out in this problem by the symmetry of the function with respect to polar angle. Thus the equation is approximated by

$$(\nabla^2 U)_1 = \frac{2}{k^2} (U_a - 2U_1 + U_b) + \frac{1}{h^2} (U_r - 2U_1 + U_\ell) \quad (3)$$

If we enumerate each lattice point as in Fig. 1 and assume the boundary values as follows:

at lattice points 12, 24, 36, 48, 60-70	$U = 0$
23	$U = 400$
35	$U = 300$
47	$U = 200$
59	$U = 100$
1-11	$U = 0$ (see Sub-appendix)

then, from equations (2) and (3), one obtains a set of 40 linear simultaneous equations with 40 unknowns. The equations (2) and (3) may be put into relaxation form (i.e., the coefficient of  $U_1$  equals -1), and summed up in one equation:

$$G(J)(\nabla^2 U)_1 = C(J)U_a + D(J)U_b + E(J)(U_r + U_\ell) - U_1 = R_1 \quad (4)$$

where  $C(J)$ ,  $D(J)$ ,  $E(J)$ , and  $G(J)$  are sets of coefficients which

vary with the row number  $J$ , and  $R_1$  the remainder associated with this equation.

If a relaxation factor  $\omega$  is chosen, the next iteration of calculation of  $U_1$  will be

$$U_1' = \omega [C(J)U_a + D(J)U_b + E(J)(U_r + U_e)] + (1 - \omega)U_1 \quad (5)$$

which is the actual equation of calculation followed by the machine.

Programming. The program was written in Fortran language. Using For Transit II system (not the revised one), the Fortran statements were first translated to IT statements, then compiled to SOAP II program and finally assembled into Object program of machine language. These were all done automatically by the machine.

The program written in Fortran language was designed to be flexible, so that when it is desired to change convergence criterion, relaxation factor, boundary conditions, or net sizes, the program will remain unchanged. The only thing required is changing of the data cards. Unfortunately, the change of the number of lattice points could not be incorporated into the program. Some statements cards must be changed, and the resulting re-translation, recompilation, and reassembling could not be avoided.

Results. Table 1 gives the number of iterated calculation and time required for reaching solutions of different degrees of accuracy at different values of relaxation factor. The  $N-\omega-S_c$  curves and discussion were presented previously.

Table 1. N- $\omega$ - $S_c$  relation.

$S_c$	$\omega = 0.8$		$\omega = 1.0$		$\omega = 1.2$		$\omega = 1.4$		$\omega = 1.6$		$\omega = 1.8$	
	N	T	N	T	N	T	N	T	N	T	N	T
0.1	34	14	25	12	19	9	14	6	21	9	41	17
0.01	50	21	36	15	26	11	17	8	24	11	50	21
0.001	67	28	47	19	32	14	20	9	29	13	59	25
0.0001	84	33	58	24	39	16	21	10	35	15	69	30

$S_c$  = degree of accuracy or convergence criterion  
 N = number of iterated calculations  
 T = time required in minutes  
 $\omega$  = relaxation factor

For various lengths of the tube, it was found that the optimum over-relaxation factor remained essentially constant. Results in Table 2 were obtained for accuracy  $S_c = 0.00001$ .

Another result was obtained for  $d = 10$  cm, but  $k' = k/2$  and  $h' = h/2$  (344 internal lattice points). Using  $\omega = 1.4$ , 65 iterations were required. For this particular problem, since the value of the function died out rapidly along z-direction, the increase of lattice points horizontally did not affect the number of iterated calculations required. By doubling the row number, the iteration number required was also doubled.

The solution of Laplace's equation in terms of the electrostatic potential distribution was given in sub-Appendix D.

The time required for each iteration of calculation was about 24.3 seconds. The last iteration required about 30 seconds. Each iteration contained about 2500 machine instructions; thus the machine roughly executed 100 instructions per second.

Table 2. d- $\omega$ -N relation.

d (cm)	No. of interior points	$\omega$	N
5	40	1.38	26
5	40	1.39	24
5	40	1.40	24
5	40	1.41	24
5	40	1.42	24
5	40	1.43	25
10	84	1.38	35
10	84	1.39	33
10	84	1.40	32
10	84	1.41	31
10	84	1.42	31
10	84	1.43	31
10	84	1.44	32
15	128	1.38	36
15	128	1.40	35
15	128	1.41	35
15	128	1.43	35
15	128	1.45	36
20	172	1.38	36
20	172	1.42	35
20	172	1.46	37
30	260	1.38	36
30	260	1.42	35
30	260	1.46	37



**SUB-APPENDICES**

## SUB-APPENDIX A

Detail of Derivation of the  
Equation of Calculation

By definition of central difference,

$$\begin{aligned} \left(\frac{\partial U}{\partial r}\right)_i &= \frac{1}{k}(U_{a/2} - U_{b/2}) = \frac{1}{2k}(U_a - U_b) \\ \left(\frac{\partial^2 U}{\partial r^2}\right)_i &= \frac{1}{k} \frac{\partial}{\partial r}(U_{a/2} - U_{b/2}) \\ &= \frac{1}{k} \left[ \frac{1}{k}(U_a - U_1) - \frac{1}{k}(U_1 - U_b) \right] \\ &= \frac{1}{k^2}(U_a - 2U_1 + U_b) \end{aligned}$$

where subscript a designates the lattice point directly above i, b directly below i.

Similarly,

$$\left(\frac{\partial^2 U}{\partial z^2}\right)_i = \frac{1}{k^2}(U_r - 2U_1 + U_l)$$

where r designates the lattice point to the right of i,  $l$  to the left of i.

Thus we have equations (2) and (3), where we have omitted the error term which is of the order  $h^2$  or  $k^2$  (since  $h \sim k$ ).

In this program,  $l = 5$  cm

$a = 1.83$  cm

$N_c = 12$  (number of columns of lattice points)

$N_r = 6$  (number of rows of lattice points)

Hence  $h = 0.4545$  cm

$k = 0.4575$  cm

For the second or the center line row

$$\begin{aligned} (\nabla^2 U)_1 &= \frac{2}{k^2}(U_a - 2U_1 + U_b) + \frac{1}{h^2}(U_r - 2U_1 + U_l) \\ &= \frac{2}{k^2}(U_a + U_b) + \frac{1}{k^2}(U_r + U_l) - 2\left(\frac{2h^2 + k^2}{h^2 k^2}\right)U_1 \end{aligned}$$

$$\begin{aligned} R_1 &= \frac{h^2 k^2}{2(2h^2 + k^2)} (\nabla^2 U)_1 = \frac{2h^2}{2h^2 + k^2} (U_a) + \frac{0}{2h^2 + k^2} U_b \\ &\quad + \frac{k^2}{2(2h^2 + k^2)} (U_r + U_l) - U_1 \end{aligned}$$

$$\begin{aligned} U_1' &= U_1 + \omega R_1 = \omega \left[ \frac{2h^2}{2h^2 + k^2} (U_a) + \frac{k^2}{2(2h^2 + k^2)} (U_r + U_l) \right] \\ &\quad + (1 - \omega)U_1 \\ &= \omega \left[ C(1)U_a + D(1)U_b + E(1)(U_r + U_l) \right] + (1 - \omega)U_1 \end{aligned}$$

where  $C(1) = \frac{2h^2}{2h^2 + k^2} = 0.664$

$$D(1) = 0$$

$$E(1) = \frac{k^2}{2(2h^2 + k^2)} = 0.168$$

Since the first row consists of a row of boundary points, if they actually represent the row one  $k$  distance on the other side of the center line, these boundary values will change and will be equal to the third row function values at each iteration. This requires a set of additional program statements inside the iteration loop. Since the program statements inside the iteration loop should be kept minimum to save machine time, this is

not advisable. In this program, the function value on this row is set to zero all the time, and incorporated  $U_b$  into  $U_a$ . Thus in the above equation  $U_b$  is the actual  $U_b$  value, but  $\underline{U}_b$  is equal to zero.

For the third, fourth, and fifth rows:

$$\begin{aligned} (\nabla^2 U)_1 &= \frac{1}{k^2}(U_a - 2U_1 + U_b) + \frac{1}{(J-1)k} \frac{U_a - U_b}{2k} \\ &\quad + \frac{1}{h^2}(U_r - 2U_1 + U_\ell) \\ &= \frac{1}{k^2} \left[ 1 + \frac{1}{2(J-1)} \right] U_a + \frac{1}{k^2} \left[ 1 - \frac{1}{2(J-1)} \right] U_b \\ &\quad + \frac{1}{h^2}(U_r + U_\ell) - 2 \left( \frac{h^2 + k^2}{h^2 k^2} \right) U_1 \end{aligned}$$

$$\begin{aligned} R_1 &= \frac{h^2 k^2}{2(h^2 + k^2)} (\nabla^2 U)_1 = \frac{h^2}{2(h^2 + k^2)} \left[ 1 + \frac{1}{2(J-1)} \right] U_a \\ &\quad + \frac{h^2}{2(h^2 + k^2)} \left[ 1 - \frac{1}{2(J-1)} \right] U_b + \frac{k^2}{2(h^2 + k^2)} (U_r + U_\ell) - U_1 \end{aligned}$$

$$\begin{aligned} U_1' &= U_1 + \omega R_1 \\ &= \omega \left[ C(J)U_a + D(J)U_b + E(J)(U_r + U_\ell) \right] + (1 - \omega)U_1 \end{aligned}$$

where  $2 \leq j \leq 4$ . If

$$\frac{h^2}{2(h^2 + k^2)} = x = 0.248$$

$$\text{then } C(2) = \frac{h^2}{2(h^2 + k^2)} \left[ 1 + \frac{1}{2(2-1)} \right] = (3/2)x = 0.372$$

$$C(3) = (5/4)x = 0.310$$

$$C(4) = (7/6)x = 0.289$$

$$D(2) = (1/2)x = 0.124$$

$$D(3) = (3/4) x = 0.186$$

$$D(4) = (5/6) x = 0.207$$

$$\text{and } E(2) = E(3) = E(4) = \frac{k^2}{2(h^2 + k^2)} = 0.251$$

## SUB-APPENDIX B

### Scheme of the Storage of Function Value

The lattice points are numbered in the following way. The point next to the left corner in the bottom row is numbered 1, the remaining points of the bottom row then are numbered 2, 3, 4, ... successively from left to right, then going to the next higher row continue to number the points from left to right until the next point of the right corner in the highest row. (See net diagram, Plate VI.)

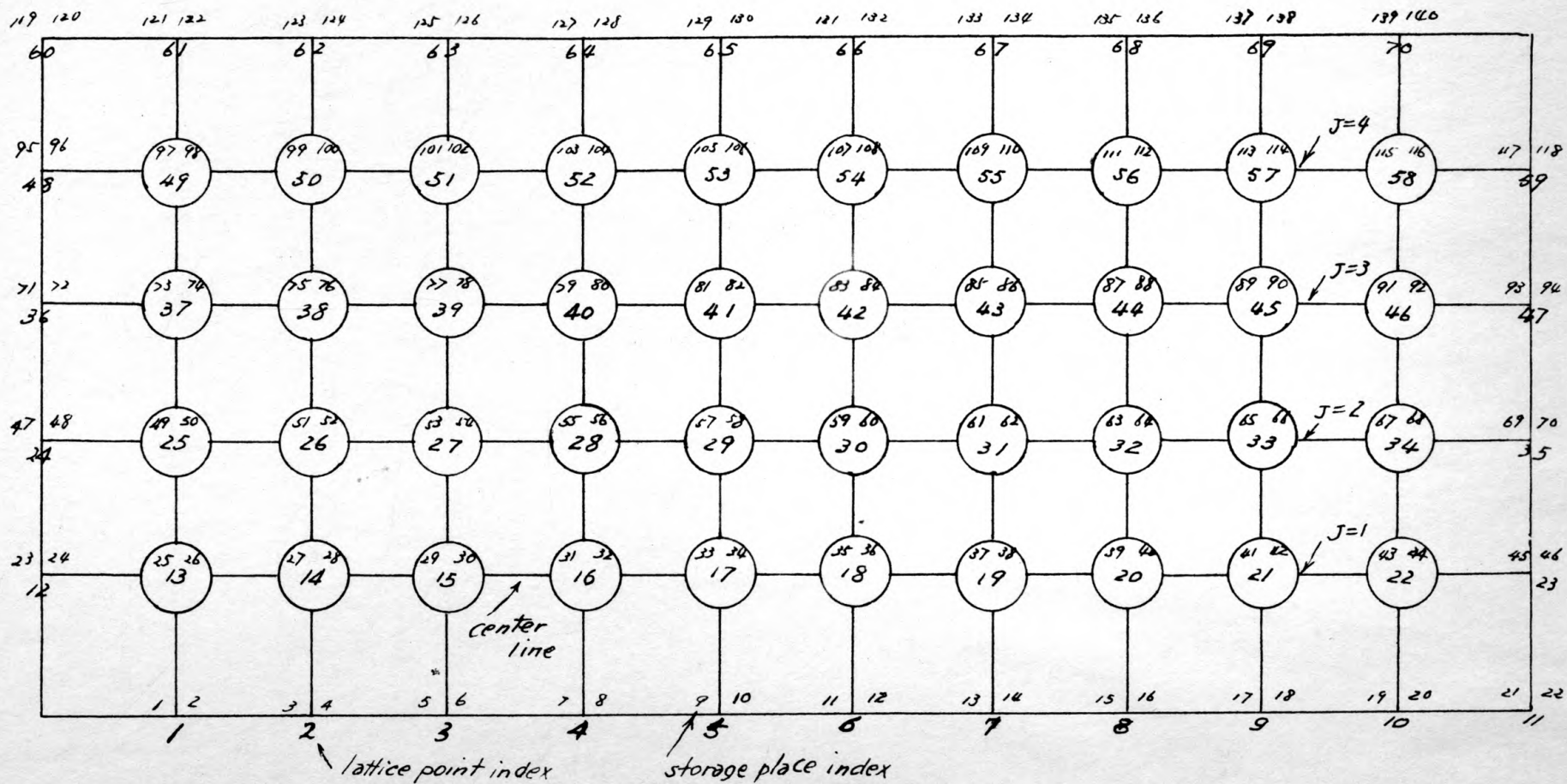
Every point is designated by two successive indexes. The  $U$  with odd index number  $U (I_{\text{odd}})$  is stored successively with the function value of the lattice point number  $(I_{\text{odd}} + 1)/2$ , calculated during each odd iteration, i.e.,  $N = 1, 3, 5, \dots$ . The  $U$  with even index number  $U (I_{\text{even}})$  is stored successively with the function value of the lattice point number  $(I_{\text{even}})/2$ , calculated during each even iteration, i.e.,  $N = 2, 4, 6, \dots$

After every iteration of calculation, there is a convergence test loop (see sub-Appendix C) to compare each containing<sup>t</sup> of the odd indexed storage place with that of the following even index,

EXPLANATION OF PLATE VI

Net diagram.

PLATE VI



i.e., to test whether or not the two successive calculations for each lattice point has converged to the accuracy required. If not, the next iteration resumes; otherwise, the results, i.e., the contents of all the indexed storage places, will be punched out by the punch statement.

If  $N$  = number of iteration

$I$  = index of  $U$

$N_c$  = number of columns of lattice points including boundary

$N_r$  = number of rows of lattice points including boundary

are given, then the underlined constants in Sub-Appendix C may be calculated as follows:

$I_s = 2 N_c + I$ , starting index of calculation for odd iteration

$I_f = 2 [N_c \times (N_r - 1) - 2]$ , ending index of calculation for even iteration

$I_{max} = 2(N_c \times N_r - 2)$ , maximum index used

$I_{b1} = I_L + N_b$

$= I_L = 2(N_c - 2)$ , first boundary point index

$I_{bL} = I_{b1} + 2(J_{max} - 2)N_c + 2$ , last boundary point index

$J_{max} = N_r - 2$ , maximum interior row number

If  $I$  is odd, it is better efficiency to use the newer values of  $U_a$ ,  $U_b$ ,  $U_r$ ,  $U_l$ , and  $U_i$  for calculating  $U_i'$ .

In the diagram of Fig. 2, the underlined indices are used.

Thus



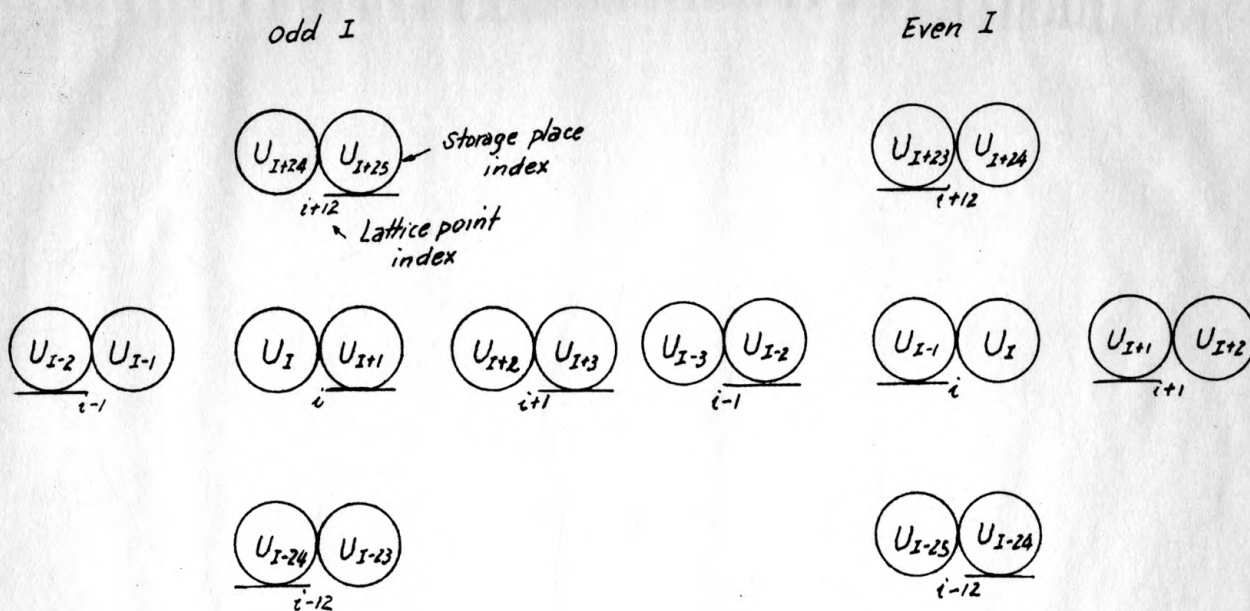


Fig. 2. Storage diagram.

$$U'(I) = \omega \left\{ CU(I + 25) + DU(I - 24) + E [U(I + 3) + U(I - 2)] \right\} + (1 - \omega) U(I + 1)$$

Similarly, if  $I$  is even, from the storage diagram,

$$U'(I) = \omega \left\{ CU(I + 23) + DU(I - 24) + E [U(I + 1) + U(I - 2)] \right\} + (1 - \omega) U(I - 1)$$

For odd  $N$ , calculate all odd indices; otherwise the even ones.

The above two equations can be combined into one:

$$U'(I) = \omega \left\{ CU(L + 24) + DU(I - 24) + E [U(L + 2) + U(I - 2)] \right\} + (1 - \omega) U(L)$$

if  $K = (-1)^N$

and  $L = I - K$ .

This is the equation used in the program.

## SUB-APPENDIX C

## Fortran Program of the Laplace Equation

```

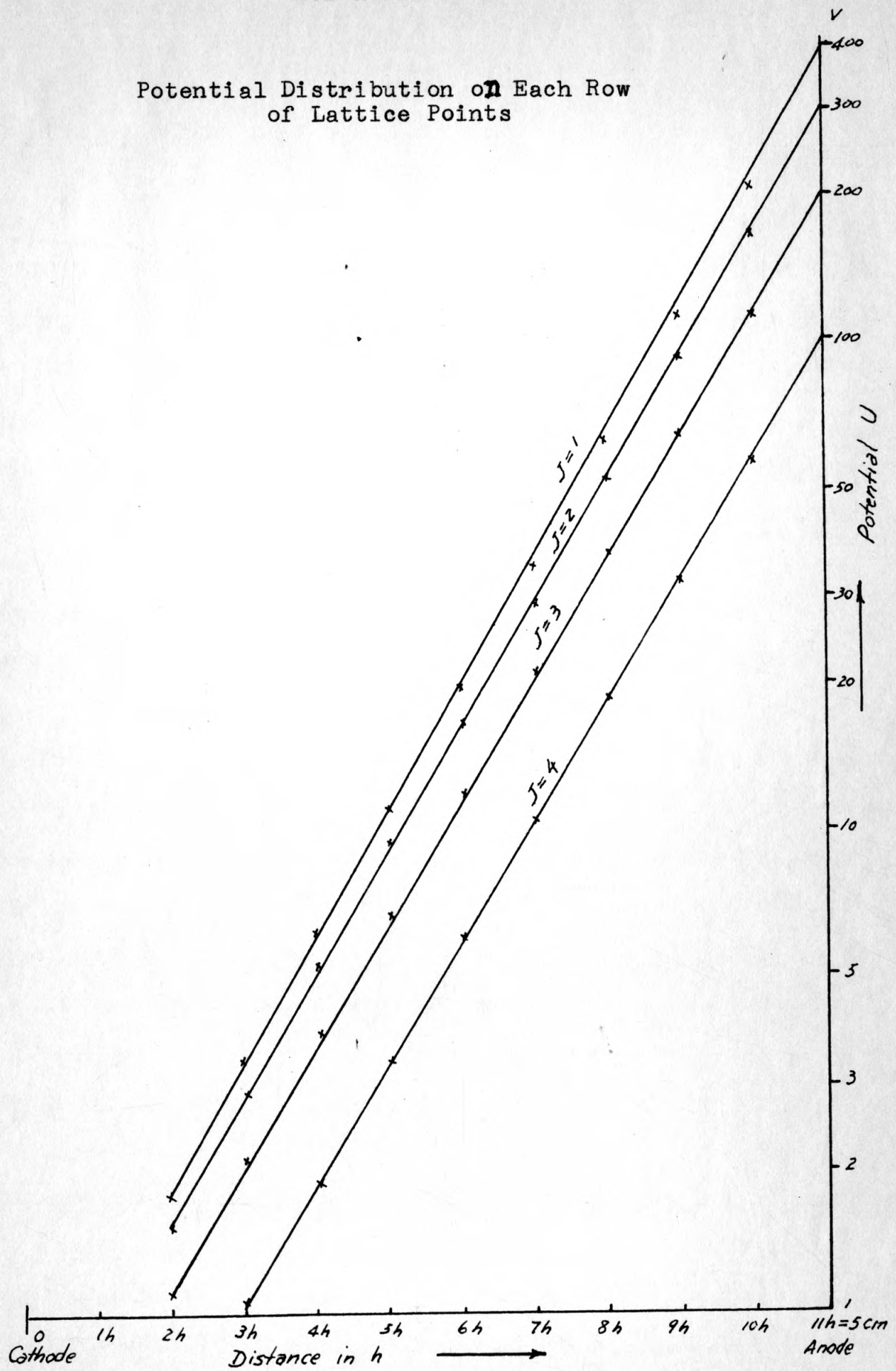
000000 LA PLACE EQUATION
000000 DIMENSION U(Imax),
          C(Jmax),D(Jmax),
          E(Jmax),S(4)
000000 READ (IWI,IWL,IWS,T)
000010 DØ14 IW=IWI,IWL,IWS
000020 DØ14 IC=1,4
000030 DØ4 I=1,Imax
000040 U(I)=0.0
000000 READ (C,D,E,S,Ub;Ub;...)
000000 N=0
000050 N=N+1
000000 PUNCH,N
000000 IL=Is
000000 K=(-1)**N
000000 IF(K)7,15,6
000060 IL=IL+1
000070 DØ10 I=IL,If,2
000080 M=I-IL-Nb
000000 Q=M*(M-2)*(M-2Nc)*
          (M-2Nc-2)*...*(M-(Jmax
          -2)*2Nc)*(M-(Jmax-2)*
          2Nc-2)
000000 IF(Q)9,10,9
000090 J=I/2Nc
000000 L=I-K
000000 V=C(J)*U(L+2Nc)+D(J)
000001 *U(I-2Nc)
000000 Y=(V+E(J)*(U(L+2)+
000001 U(I-2)))*IW/T
000000 U(I)=Y+(1-IW/T)*U(L)
000100 CØNTINUE
000000 DØ12 I=Is,If,2
000110 R=U(I+1)-U(I)
000000 IF(S(IC)-ABS(F(R)))5,
000001 12,12
000120 CØNTINUE
000130 PUNCH,U
000140 CØNTINUE
000000 GØ TØ 1
000150 STØP

```

N.B. The underlined items are calculated according to sub-appendix B.

## SUB-APPENDIX D

Potential Distribution on Each Row  
of Lattice Points



## SUB-APPENDIX E

## Remarks

1. In designing a program, the first requirement is that the program should solve the problem. The second is that the program be flexible. One wishes to design a program that can be used for various situations. This is especially true in using the For Transit system, since the translation, compilation, and assembling alone will consume a great deal of machine time. Flexibility is actually a long-range machine-time-saving plan. The third requirement is simplicity. This provides two advantages: ease of checking and less probability of error, and machine-time saving. Especially in an iterated calculation, the instruction within an iteration loop should be carefully designed to reduce the operation to a minimum. Sometimes a superficially complicated Fortran statement when processed to an object program, contains fewer instructions than the seemingly simple one. Knowledge of the inside structure of the For Transit system (i.e., IT language, SOAP II language) proves to be of great help in this respect. This knowledge also helps to locate the trouble when there is a mistake in the original program.

As an example of flexibility, the change of relaxation factor incorporated in the program is explained below. Through data cards, three integers, IWI, IWL, and IWS, and a floating point constant T, are read in. The choice of these four constants to cover various relaxation factors can be easily understood by

an example. In this program, the desired relaxation factor values are:

$$\omega = 0.8, 1.0, 1.2, 1.4, 1.6, 1.8$$

If we choose

$$IWI = 8, IWL = 18, IWS = 2, T = 10.0$$

then  $IW/T$  in the  $\omega$  iteration loop will successively take the desired values of  $\omega$ . So  $IW/T$  may be used in place of  $\omega$ .

2. The net size constants  $h$  and  $k$  should be approximately equal. Otherwise, the error term in

$$\frac{\partial^2 U}{\partial z^2} = \frac{1}{h^2} (U_r - 2U_1 + U_l) + e(h^2)$$

may be large enough to upset the whole equation. Thus if  $h$  is many times greater than  $k$ , then

$$(\nabla^2 U)_i = \frac{\partial^2 U}{\partial r^2} + \frac{\partial^2 U}{\partial z^2}$$

is approximated by

$$(\nabla^2 U)_i = \frac{1}{k^2} (U_a - 2U_1 + U_b) + \frac{1}{h^2} (U_r - 2U_1 + U_l)$$

The omitted  $e(h^2)$  term may be comparable with  $\frac{1}{k^2} (U_a - 2U_1 + U_b)$ .

Hence in this approximation the role of  $\frac{\partial^2 U}{\partial r^2}$  is actually masked by the error term.

3. One may avoid many troubles by breaking long calculation statements, using intermediate variables. This does not necessarily increase the number of the ultimate machine instructions.

4. The set of simultaneous equations in this particular problem has a special character. The  $U$  values of the lattice

points die out rapidly (exponentially) from right to left because of the boundary conditions. Hence, for example, for  $S_c = 0.0001$ ,  $\omega = 1.4$ , at lattice point 22, the values of two successive calculations are

206.43928      and      206.43928

which are accurate to the eighth significant figure. But at the lattice point 13, the values are

0.76080300      and      0.76074310

which are only accurate to the fourth significant figure.

In using the IBM 650, significant figures are limited to eight for floating point variables or constants. Hence beyond a certain column on to the left (if there are enough columns), the U values are entirely unreliable. Therefore it is useless to increase the length of the tube to beyond 30 cm. Besides, in using the For Transit system, the index number is limited to below 1000, and the total storage space of the IBM 650 is only 2000 words. Thus the best accurate convergence criterion one can use is 0.00001.

THEORETICAL COMPUTATION OF THE CHARACTERISTIC  
CURVE OF THE A-C GASEOUS DISCHARGE  
IN AN ELONGATED TUBE

by

CHUNG YOW WANG

B. S., National Taiwan University,  
Taiwan, China, 1952

-----

AN ABSTRACT OF  
A MASTER'S THESIS

submitted in partial fulfillment of the

requirements for the degree

MASTER OF SCIENCE

Department of Electrical Engineering

KANSAS STATE UNIVERSITY  
OF AGRICULTURE AND APPLIED SCIENCE

1959

A boundary value problem was set up based on the major fundamental processes and the practical situations for the a-c discharge in gases in an elongated tube. The objective was to compute the characteristic curve of the discharge about the glow region. This boundary value problem was solved numerically, using the method of finite differences. The entire computing procedures were coded in Fortran language which was readily adapted for use in both the IBM 650 and the 704 computers. The preliminary test of the major and time-consuming part of the program--Laplace's equation in cylindrical coordinates--has been solved in order to find the relation between relaxation factor and the number of scanning iterations of computation. The optimum over-relaxation factor for this particular program was nearly 1.4. The characteristic curve of the discharge has not yet been obtained. Further adjustment of the constants used in the computation and possible improvement of the boundary conditions to take care of the mobility effect at the boundaries were needed. Additional work is planned to improve the results presently obtained.